Electronic Supplementary Information

Graphene-encapsulated nickel-copper bimetallic nanoparticle catalysts for electrochemical reduction of CO_2 to CO

Chaochen Xu,[a] Anthony Vasileff,[a] Bo Jin,[a] Dan Wang,[b] Haolan Xu,[c] Yao Zheng*[a], and Shi-Zhang Qiao*[a]

[a] Centre for Materials in Energy and Catalysis, School of Chemical Engineering and Advanced Materials, The University of Adelaide, Adelaide, SA 5005, Australia

[b] Institute of Process Engineering, Chinese Academy of Sciences, Beijing, 100190, China

[c] Future Industries Institute, University of South Australia, SA 5095, Australia

* Email: s.qiao@adelaide.edu.au, yao.zheng01@adelaide.edu.au

Part I: Experimental Section

Chemicals

Nickel(II) nitrate hexahydrate ($Ni(NO_3)_2 \cdot 6H_2O$), copper(II) nitrate hemi-pentahydrate ($Cu(NO_3)_2 \cdot 2.5H_2O$), ethylenediaminetetraacetic acid (EDTA), *N,N*-dimethylformamide (DMF), trimethylamine (TMA), potassium bicarbonate ($KHCO_3$), dimethyl sulfoxide (DMSO), phenol, and deuterium oxide (D_2O) were purchased from Sigma-Aldrich and were used without further purification. Deionized water (DI water, 18 MΩ·cm) was from a Milli-Q water purifier. A 0.05 wt.% Nafion solution was diluted from LIQUion™ Solutions (LQ-1115 - 1100 EW at 15 wt.%). Ultra-high purity Ar (99.999%), N_2 (99.999%), and laser grade CO_2 (99.995%) were supplied from BOC Gas.

Synthesis Method

NiCu bimetallic nanoparticles were prepared using a modified method.[1] 0.6 g of EDTA and 1.0 mL of TMA were dissolved in 30 mL DMF and formed EDTA solution. The bimetallic salt solution was prepared by dissolution of specific ratios of nickel(II) and copper(II) nitrate salts in 20 mL DMF. For example, 1.4 g of the Ni salt and 0.3 g of the Cu salt were used for the preparation of $NiCu_{0.25}$ salt solution. For $NiCu_{0.5}$ and NiCu salt solution, 1.2 and 0.9 g of the Ni salt and 0.5 and 0.7 g of the Cu salt were used, respectively. The bimetallic salt solution was then added dropwise to the EDTA solution under vigorous stirring. A clear gelatinous precipitate was received after washing with DMF three times by centrifugation (6000 rpm). The washed precipitate was dried in a vacuum oven at 80°C overnight. The fully dried resultant was transferred to a tube furnace and was annealed at 550°C with a heating rate of $10°C \cdot min^{-1}$ for 1 h under Ar atmosphere. Once cooled to room temperature, the received black powder was washed with DI water three times and was dried in a vacuum oven at 60°C overnight again. For comparison, single Ni or Cu nanoparticles were synthesized using the same method by adding 1.7 g of the Ni salt or 1.4 g of the Cu salt only.

Material Characterization

Scanning electron microscopy (SEM) images and energy dispersive spectroscopy (EDS) spectra were acquired with FEI Quanta 450. Transmission electron microscopy (TEM) images and selected area electron diffraction (SAED) patterns were taken using Philips CM200. High-angle annular dark-field scanning transmission electron microscopy (HAADF-STEM) images and EDS spectra were acquired with FEI Titan Themis 80-200. X-ray powder diffraction

(XRD) patterns were recorded on a Rigaku X-Ray Diffractometer (Cu Kα, λ = 1.5406 Å). X-ray photoelectron spectroscopy (XPS) measurements were performed on Kratos AXIS Ultra (mono Al Kα), and all spectra were calibrated to the C-C peak at 284.8 eV. X-ray absorption spectra were collected from the soft X-ray spectroscopy (sXAS) and X-ray absorption spectroscopy (XAS) beamlines at the Australian synchrotron. All spectra were calibrated by corresponding reference standards of metal foils (Cu K-edge at 8978.9 eV, Ni L_3-edge at 853.0 eV, and Cu L_3-edge at 934.3 eV). The position of the absorption edge was determined from the first derivatives of the spectrum. X-ray absorption near edge structure (XANES) and extended X-ray absorption fine structure (EXAFS) data processing was conducted in Athena. Raman spectra were collected using a Raman spectroscopy (HORIBA LabRAM HR Evolution) configured by an MPLN50x objective lens (Olympus) and a 633-nm laser (CVI Melles Griot).

Electrochemical Measurements

The experiments were performed on an electrochemical workstation (CH Instruments 760E) using a three-electrode H-cell separated by a proton exchange membrane (Nafion 117). A glassy carbon electrode (⌀ 5 mm), Ag/AgCl (3.5 M KCl), and RuO_2-coated titanium mesh served as the working, reference, and counter electrodes, respectively. To prepare a catalyst ink, 4 mg of catalyst was ultrasonically dispersed in 2 mL of 0.05 wt.% Nafion aqueous solution. Then, 40 μL of the ink was dropped onto the surface of the glassy carbon and dried in air, resulting in a catalyst loading of 0.4 $mg \cdot cm^{-2}$. The electrochemical measurements including cyclic voltammetry (CV), linear scan voltammetry (LSV), and chronoamperometry *i-t* curve (*i-t*) were carried out in CO_2-saturated 0.1 M $KHCO_3$ electrolyte (pH = 6.8) under a stirring rate of 100 rpm. All *iR*-corrected potentials were converted to the reversible hydrogen electrode (RHE) at 20°C:

$$E\ (V\ vs.\ RHE) = E\ (V\ vs.\ Ag/AgCl) + 0.059 \times pH + 0.205$$

where *pH* is measured using a pH meter.

For the analysis of electrochemical kinetics, Tafel slopes were derived from the Tafel equation:

$$\eta = b\ lg\ (j_{CO} / j_0)$$

where η [V] is an overpotential between the applied potential to the standard CO_2/CO reduction potential ($E_{CO2/CO}$ = -0.11 V *vs.* RHE); *b* is the Tafel slope [$mV \cdot dec^{-1}$]; j_{co} is the partial current density of CO; j_0 is the exchange current density of CO [$mA \cdot cm^{-2}$].

Product Evaluation

Briefly, 100 μL of headspace gas in the cathode compartment was manually injected into gas chromatography (GC, Agilent 7890B configured with TCD and Methanizer/FID) for gas product quantification *via* a syringe; The liquid products were determined using nuclear magnetic resonance spectroscopy (NMR, Agilent 500/600 MHz ^{1}H NMR) and were quantified with internal standards (DMSO and phenol in D_2O).[2] No detectable liquid products were found in this work. Faradaic efficiency of a certain product was calculated by:

$$FE_i = n_i\, e\, F / Q_t \times 100\%$$

where n_i is the total amount of a certain product i [mol]; e is the number of electrons transferred for the product i formation, which equals to two for both CO and H_2; F is the Faradaic constant [$C \cdot mol^{-1}$]; Q_t is the total amount of passed charge [C].

***In-situ* Raman Spectroscopy Measurements**

The same catalyst inks used for electrochemical measurements were also used for *in-situ* Raman spectroscopy measurements. 40 μL of catalyst ink was uniformly deposited on a 5 mm × 4 mm screen-printed working electrode (Pine Research Instrumentation, RRPE1002C). The electrode was then transferred to a vacuum oven and was dried at 60°C. The fully dried electrode was connected to the 760E electrochemical workstation *via* a cell grip and USB connector and was then attached on a microscope slide at the sample stage. 100 μL of CO_2-saturated 0.1M $KHCO_3$ electrolyte was dropwise added on the electrode. A coverslip was then placed on the top of the electrode. *In-situ* Raman spectra were collected using a Raman spectroscopy (HORIBA LabRAM HR Evolution) configured by an MPLN50x objective lens (Olympus), 1800 l/mm grating, and a 633-nm Raman laser. Baseline correction was applied in all *in-situ* Raman spectra. All applied potentials were converted to RHE at 20°C:

$$E\ (V\ vs.\ RHE) = E\ (V\ vs.\ Ag/AgCl) + 0.059 \times pH + 0.527$$

where *pH* is measured using a pH meter.

Part II: Supplementary Results

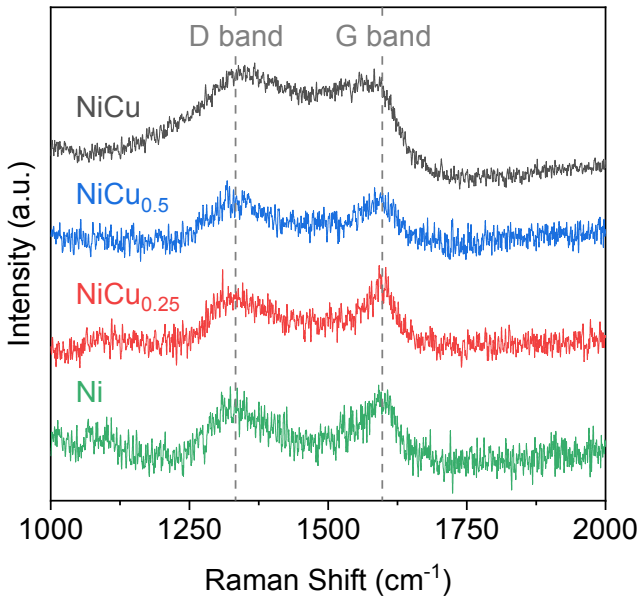

Fig. S1 Raman spectroscopy spectra. The dash lines are assigned to the D- (~1350 cm^{-1}) and G- (~1580 cm^{-1}) band peaks.

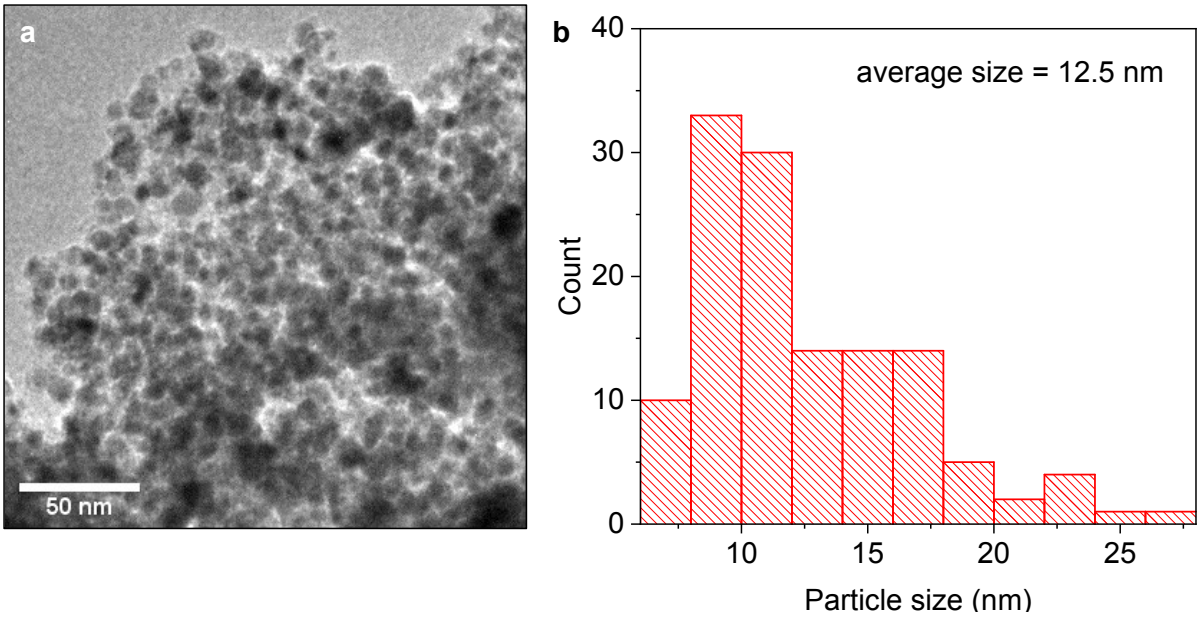

Fig. S2 (a) TEM image of $NiCu_{0.25}$ and (b) its corresponding particle size distribution.

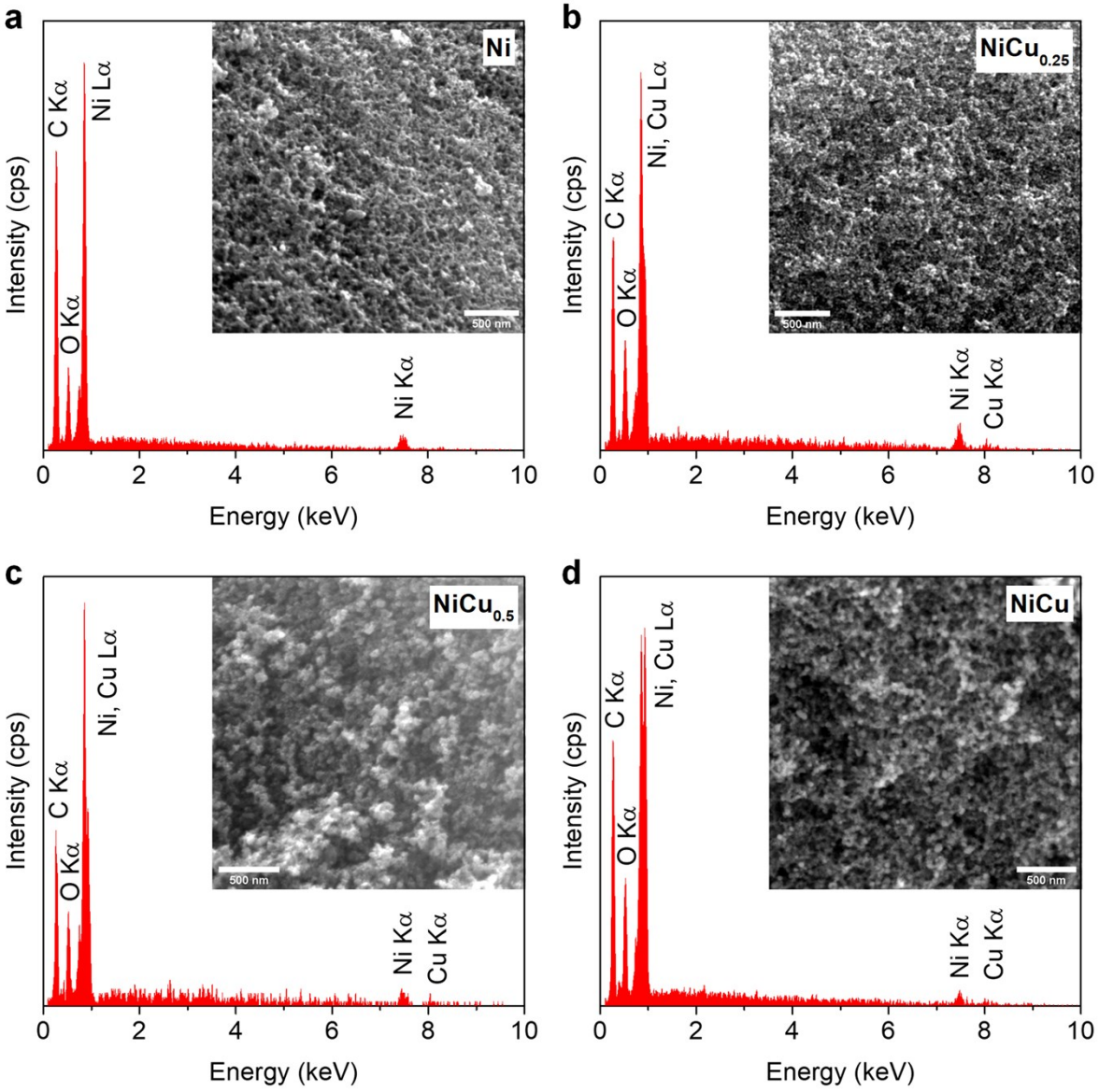

Fig. S3 SEM images (inset) and corresponding EDS elemental analysis of (a) Ni, (b) $NiCu_{0.25}$, (c) $NiCu_{0.5}$, and (d) NiCu (scale bars = 500 nm).

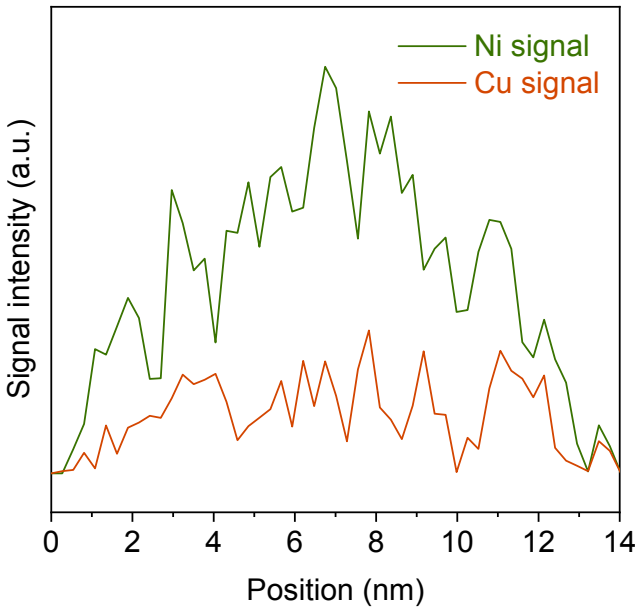

Fig. S4 EDS line scan of $NiCu_{0.25}$ along the arrowed direction in Fig. 1(b).

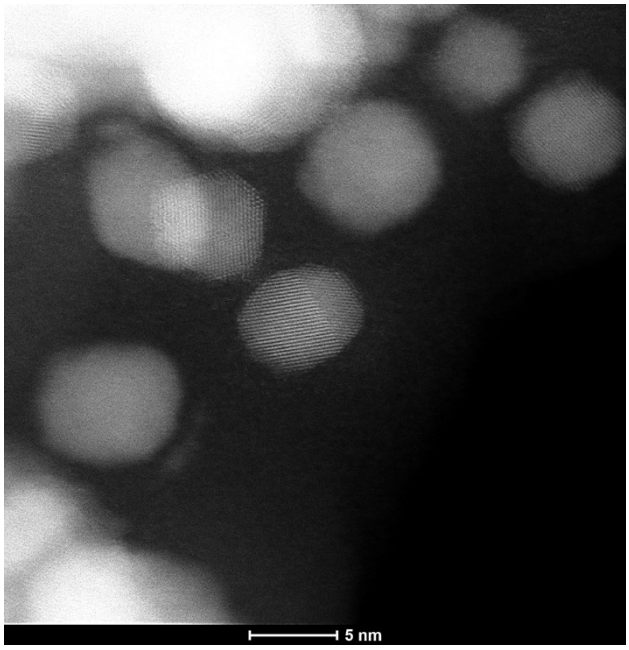

Fig. S5 HAADF-STEM images of Ni-Cu bimetallic nanoparticle catalysts.

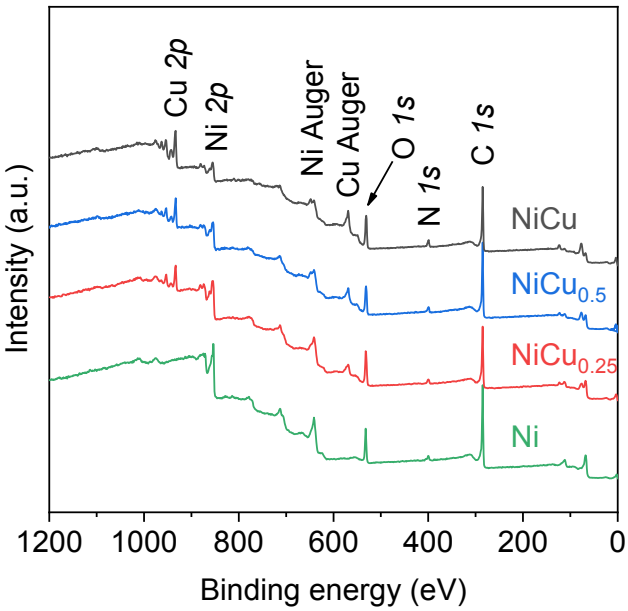

Fig. S6 XPS survey spectra with distinct signals of C, N, O, Ni, and Cu.

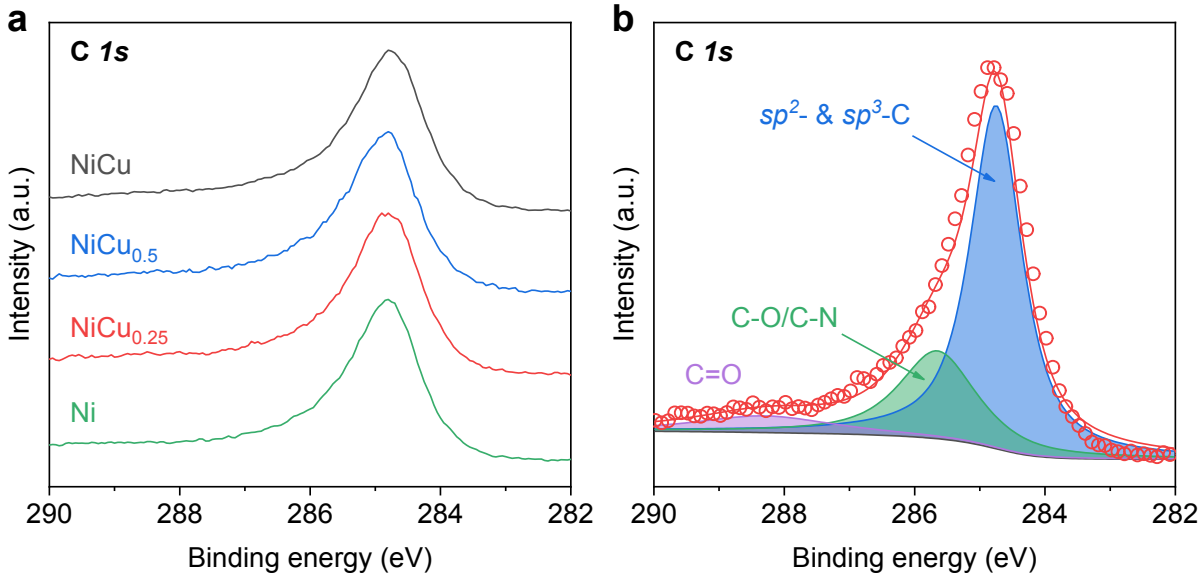

Fig. S7 High-resolution XPS spectra of (a) C 1s and (b) the deconvoluted spectrum of $NiCu_{0.25}$.

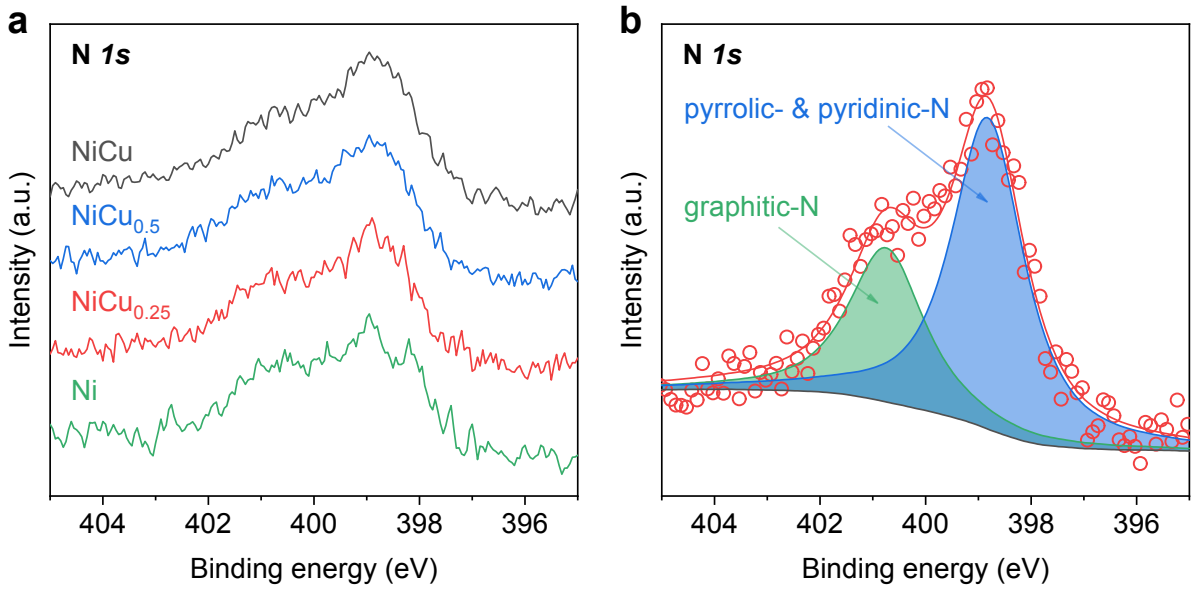

Fig. S8 High-resolution XPS spectra of (a) N 1s and (b) the deconvoluted spectrum of $NiCu_{0.25}$.

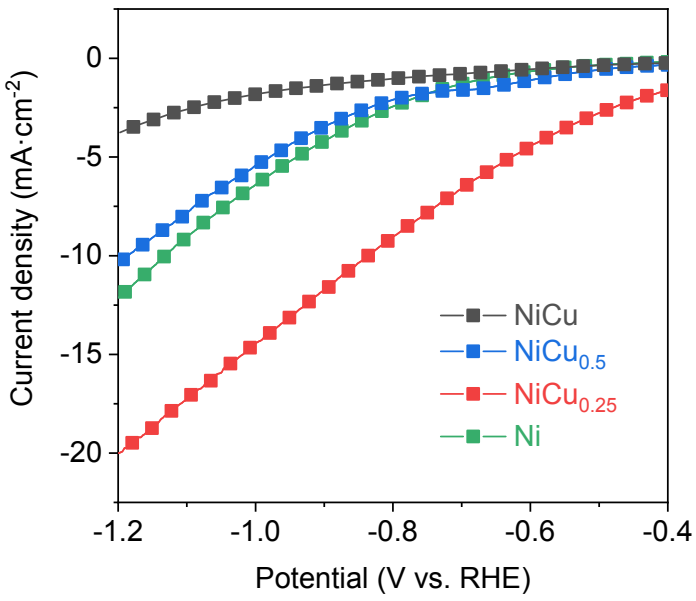

Fig. S9 LSV polarization curves in CO_2-saturated 0.1 M $KHCO_3$ electrolyte.

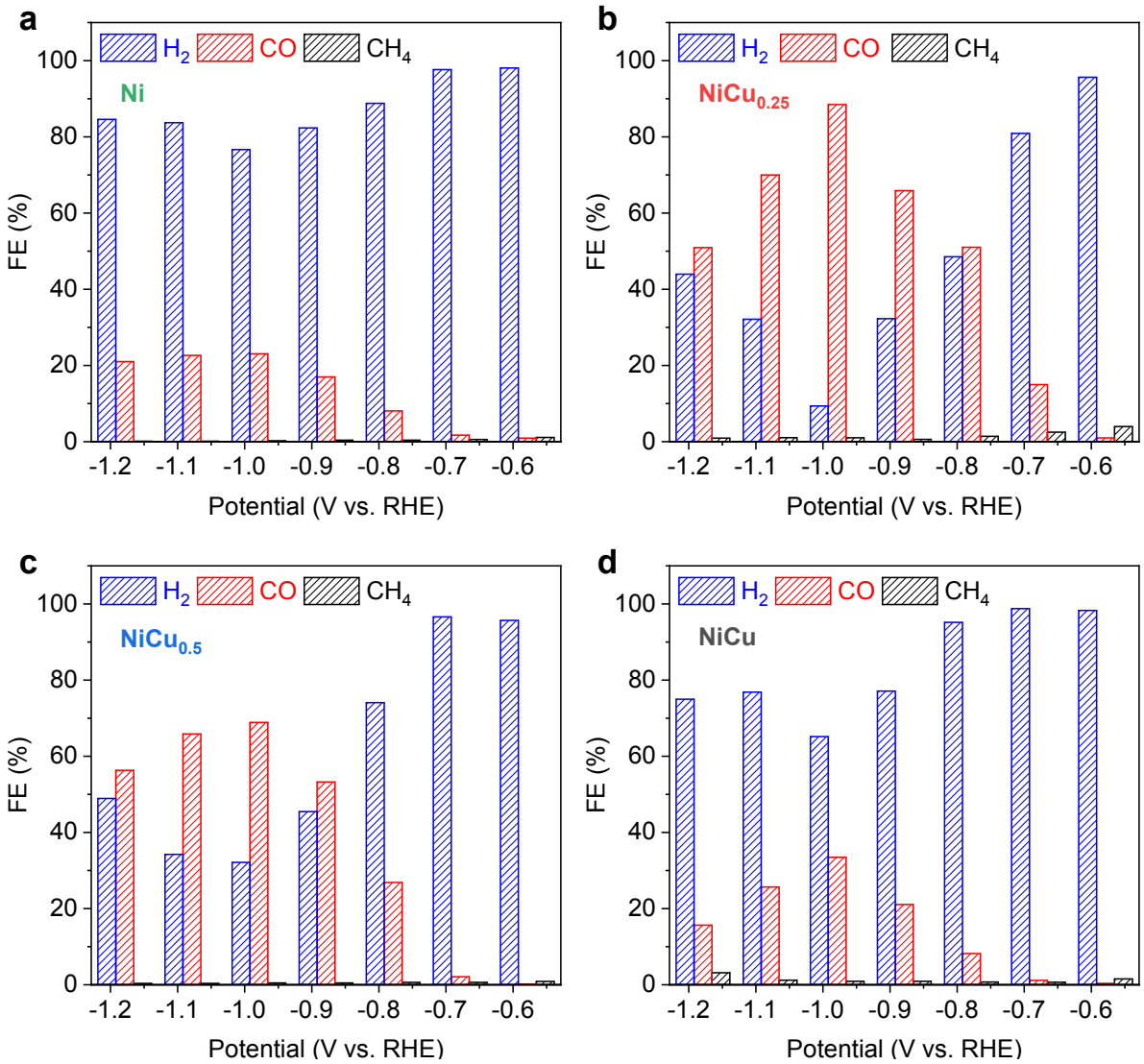

Fig. S10 Measured FE distributions of CO_2 electroreduction on (a) Ni, (b) $NiCu_{0.25}$, (c) $NiCu_{0.5}$, and (d) NiCu in CO_2-saturated 0.1 M $KHCO_3$ electrolyte.

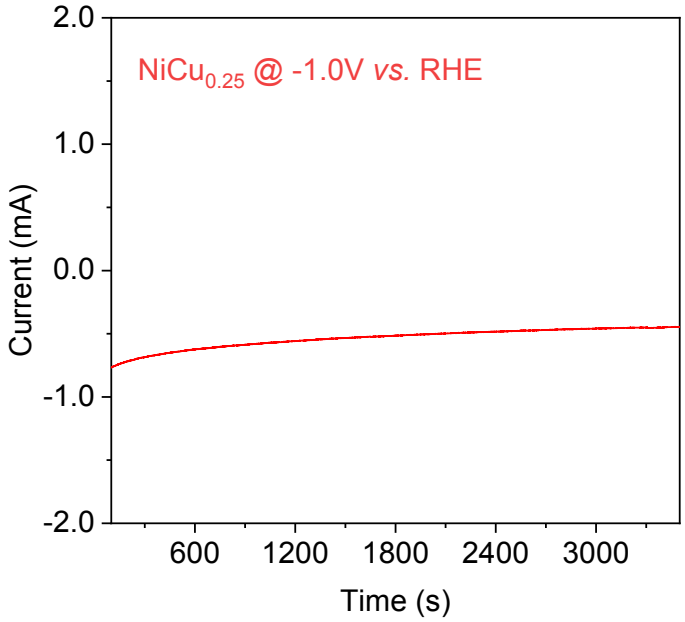

Fig. S11 Current-time dependence of $NiCu_{0.25}$ for CO_2 electroreduction in CO_2-saturated 0.1 M $KHCO_3$ electrolyte at -1.0 V *vs.* RHE.

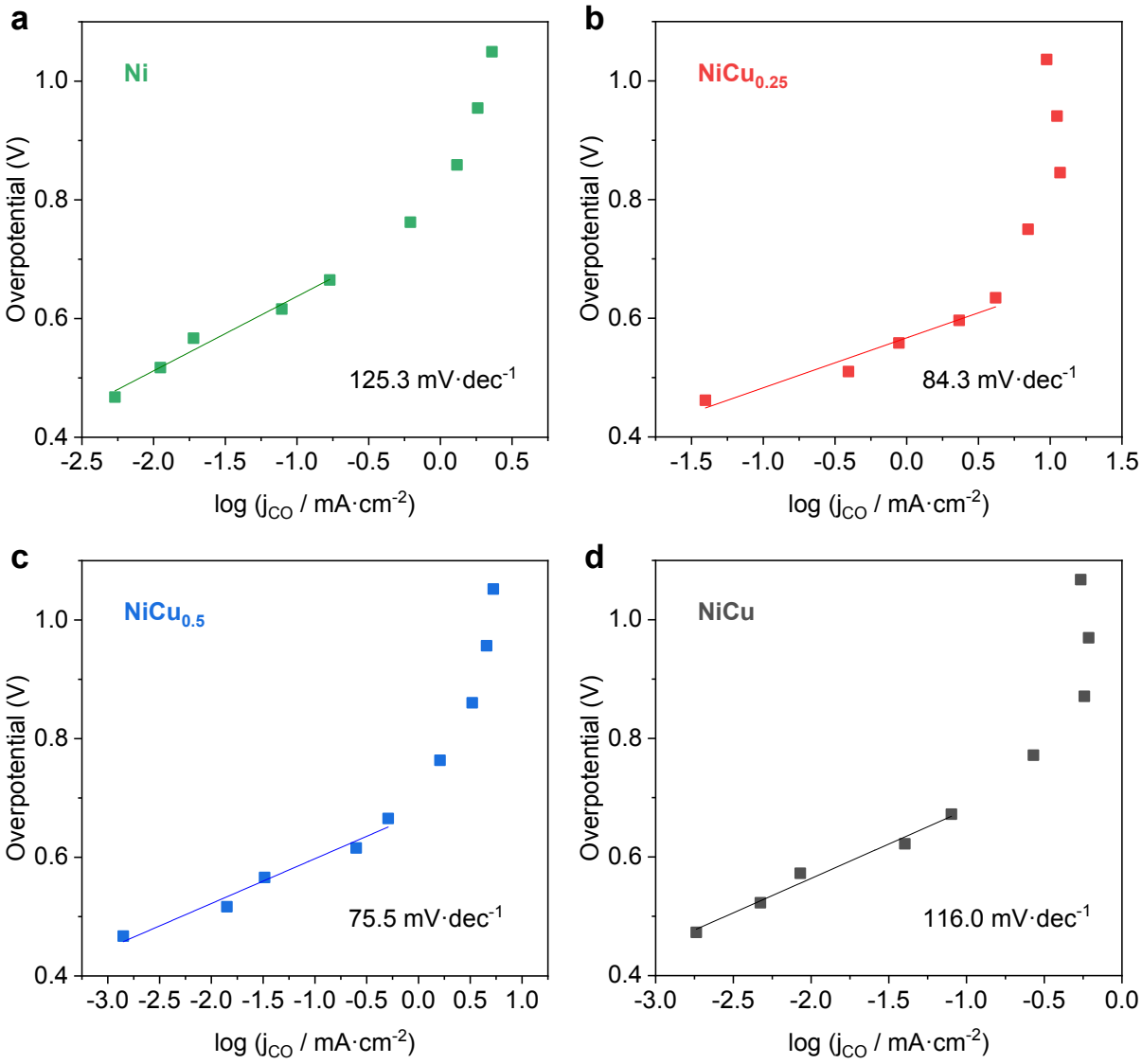

Fig. S12 Tafel plots for CO evolution on (a) Ni, (b) $NiCu_{0.25}$, (c) $NiCu_{0.5}$, and (d) NiCu in CO_2-saturated 0.1 M $KHCO_3$ electrolyte.

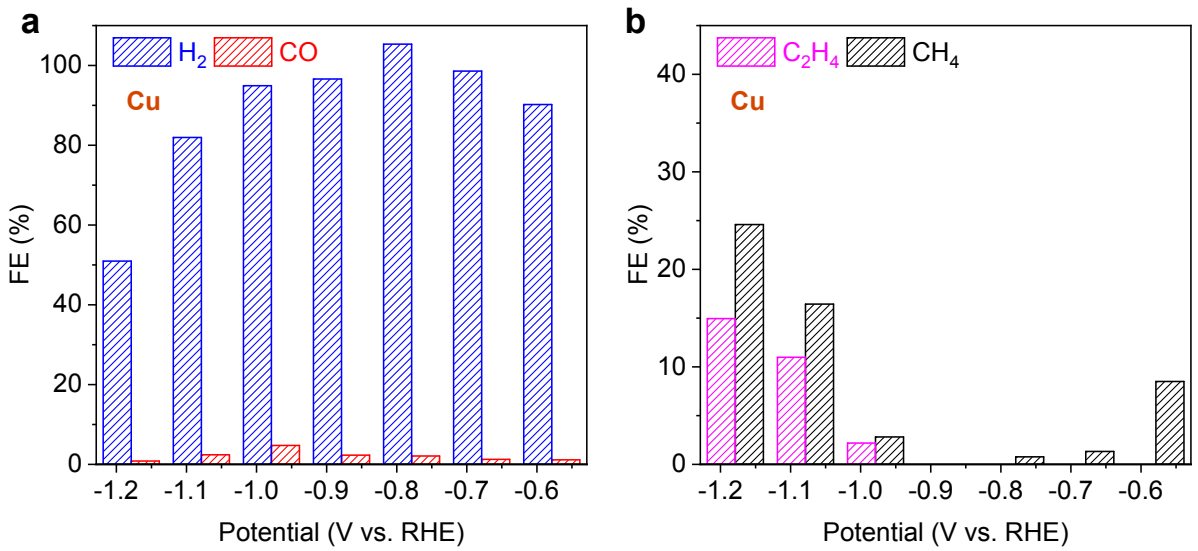

Fig. S13 Measured FEs toward (a) H_2, CO, and (b) hydrocarbons on the Cu catalyst.

Table S1. Theoretical and STEM-EDS measured atomic ratios of Cu-to-Ni.

Sample	**Atomic ratios of Cu-to-Ni**	
	Theoretical	*Measured*
NiCu	1.00	0.95
NiCu0.5	0.50	0.46
NiCu0.25	0.25	0.24
Ni	0.00	N/A

Table S2. Surface chemical composition measured by XPS

Signals	**Atomic%**			
	NiCu	*$NiCu_{0.5}$*	*$NiCu_{0.25}$*	*Ni*
C 1s	62.84	66.41	63.02	69.78
N 1s	5.5	4.82	4.17	3.93
O 1s	18.32	15.81	17.95	14.37
Ni 2p	5.5	7.67	10.61	10.52
Cu 2p	7.84	5.29	4.25	N/A

Part III: References

1. K. Zhang, J. Ran, B. Zhu, H. Ju, J. Yu, L. Song and S. Z. Qiao, *Small*, 2018, **14**, 1801705.
2. K. P. Kuhl, E. R. Cave, D. N. Abram and T. F. Jaramillo, *Energy Environ. Sci.*, 2012, **5**, 7050-7059.